

# UNDERSTANDING THE ROLE OF DIFFUSION IN THE SEPARATION OF RARE EARTH ELEMENTS IN WATER-*n*-HEXANE SYSTEMS: A MOLECULAR DYNAMICS SIMULATION STUDY

ARI HARDIANTO<sup>1\*</sup>, REGAPUTRA SATRIA JANITRA<sup>2</sup>, MUHAMMAD RYAN FAUZI<sup>1</sup>, JULIANDRI<sup>1</sup>, ANNI ANGRAENI<sup>1</sup>, AND UKUN MOCHAMMAD SYUKUR SOEDJANAATMADJA<sup>1</sup>

<sup>1</sup>Department of Chemistry, Faculty of Mathematics and Natural Sciences, Universitas Padjadjaran, Jatinangor 45363 West Java, Indonesia

<sup>2</sup>Biotechnology Master Program, Postgraduate School, Universitas Padjadjaran, Bandung 40132 West Java, Indonesia

\*Corresponding Author email: a.hardianto@unpad.ac.id

---

## Article Information    Abstract

Received: Nov 08, 2023  
Revised: Nov 30, 2023  
Accepted: Dec 23, 2023  
Published: Dec 31, 2023

DOI:  
10.15575/ak.v10i2.30680

Keywords: Rare Earth Elements (REE); Liquid-liquid extraction; molecular dynamics simulations; diffusion coefficients; ion mobility.

Liquid-liquid extraction is one of the methods for separating rare earth elements (REE) in the presence of an extractant. The separation of REE ions, complex with an extractant, involves interfacial migrations that are influenced by the diffusion of the respective ions. Therefore, we performed molecular dynamics simulations on REE ions (La<sup>3+</sup>, Sm<sup>3+</sup>, Eu<sup>3+</sup>, Gd<sup>3+</sup>, and Tb<sup>3+</sup>) in a water-*n*-hexane system to determine if each ion exhibited a distinct diffusion coefficient. By employing molecular dynamics simulations, we calculated diffusion coefficients for these ions based on the Einstein relation. The diffusion coefficients for La<sup>3+</sup>, Sm<sup>3+</sup>, Eu<sup>3+</sup>, Gd<sup>3+</sup>, and Tb<sup>3+</sup> were found to be 4.21×10<sup>-6</sup>, and 3.96×10<sup>-6</sup>, 4.57×10<sup>-6</sup>, 4.17×10<sup>-6</sup>, and 5.19×10<sup>-6</sup> cm<sup>2</sup>/s, respectively. However, statistical analysis via the Kruskal-Wallis test revealed no significant variance in the diffusion coefficients (p-value greater than 0.05), indicating that diffusion is not a rate-limiting factor in REE separation. The findings suggest that effective mixing during extraction can eliminate the role of diffusion as a differentiating factor in REE separation. Overall, this study offers critical insights into optimizing REE extraction processes.

---

## INTRODUCTION

Rare earth elements (REE) have many potential applications, including electronics, catalysis, sensors, and medicine. La<sub>2</sub>O<sub>3</sub> can enhance the specific capacitance and effective conductive area of reduced graphene oxide (RGO), making it a potential candidate for electrode material in supercapacitors [1]. The perovskite compound SmCoO<sub>3</sub> is used as a catalyst in converting methane and carbon dioxide into syngas [2]. Eu<sup>3+</sup> complexes are used as spectroscopic probes, such as luminescent probes for detecting singlet oxygen and nitric oxide [3][4]. Gd<sup>3+</sup> complexes are contrast agents in magnetic resonance imaging (MRI) [5][6][7][8]. The photocatalytic activity of ZnS quantum dots can be enhanced by doping with Tb<sup>3+</sup> [9]. Therefore, the optimization of REEs separation from ores is essential.

Liquid-liquid extraction is widely used in metal separation. A well-known example of its application is in the PUREX (plutonium uranium

reduction extraction) process, *i.e.*, separating plutonium and uranium from used nuclear fuel. Fundamentally, liquid-liquid metal extraction involves the transfer of metal ions (which are hydrophilic) from the aqueous phase to the hydrophobic organic solvent phase. The complex formation of metal ions with hydrophobic ligands is crucial in the extraction process [10][11].

Some widely used extractant ligands are tri-*n*-butylphosphate (TBP) in the PUREX process [10][11], di-2-ethylhexyl phosphoric acid (D2EHPA) for Sc<sup>3+</sup> extraction [12], bis(2,4,4-trimethylpentyl)phosphinic acid (Cyanex 272) for In<sup>3+</sup> and Ga<sup>3+</sup> extraction [13], and trialkylphosphine oxide (Cyanex 923) for REEs extraction [14]. A suitable extractant ligand should have low solubility in water, be resistant to hydrolysis, be reusable for multiple extraction cycles, and have good mixing ability with diluents [15]. However, if a suitable extractant ligand must have low water solubility, it raises the question of how complex formation between metal ions and ligands can occur. Several theoretical studies have shown that

metal ions in the aqueous phase and ligands in the organic phase migrate toward the aqueous-organic phase interface, where they subsequently react to form complexes [11][16][17]. Therefore, that reaction is diffusion-controlled because it relies on the migration of reactants (metal ions and ligands) to meet each other at the interface. As a result, the diffusion rate of metal ions in water and ligands in the organic phase significantly influences the rate of complex formation and can even affect the kinetics of extraction [18][19].

D'Angelo et al. [20] and Passler & Rode [21] have conducted molecular dynamics simulation studies of REE ions in water but have not calculated the diffusion coefficients. Therefore, to study the diffusion factors in the extraction for separating REEs among them, we calculated the diffusion coefficients of  $\text{La}^{3+}$ ,  $\text{Sm}^{3+}$ ,  $\text{Eu}^{3+}$ ,  $\text{Gd}^{3+}$ , and  $\text{Tb}^{3+}$  in water in the water-n-hexane system (two immiscible solvents). The diffusion coefficient is obtained from the molecular dynamics simulation trajectories analysis based on the Einstein relation.  $\text{La}^{3+}$  and  $\text{Sm}^{3+}$  represent light REEs, while  $\text{Eu}^{3+}$ ,  $\text{Gd}^{3+}$ , and  $\text{Tb}^{3+}$  represent heavy REEs. The Kruskal-Wallis test was carried out to evaluate a significant difference in the diffusion coefficient among those ions.

## EXPERIMENT

### *Simulation System Preparation*

The water-n-hexane system (two immiscible solvents) was prepared by Packmol [22][23] with dimensions  $100 \times 60 \times 60$  Å. There are five simulation systems. Each system consists of the same ten REE ions and 30  $\text{Cl}^-$  ions in the aqueous phase. Chloride ions were used as counter ions to neutralize the system. The solvent and ion coordinates are the same for all REEs simulation systems.

### *Molecular Dynamics Simulation*

The force field used for REE ions,  $\text{Cl}^-$ , and  $\text{H}_2\text{O}$  is TIP3P [24][25], while that for n-hexane is GAFF [26][27] with the partial charge of the atom set to 0. Minimization was carried out for 10,000 cycles using the steepest descent method. Heating from 0 to 300 K under constant volume conditions for 75 ps, followed by density equilibration for 2.5 ns at 300 K under NPT conditions. Subsequently, a mixing simulation was conducted for 0.2 ns at 500 K under constant volume conditions. A temperature of 500 K was used to model collisions

during the mixing process [11]. Production simulations were conducted for 100 ns under NPT conditions. Temperature regulation uses a Langevin thermostat, while pressure regulation uses a Berendsen barostat. Non-bonded interaction calculations were carried out using the PME method with a cutoff of 10 Å. The SHAKE algorithm for hydrogen-involved bonds was employed during the equilibration to production simulation. Five replications were carried out from the minimization stage to production. Molecular dynamics simulations were performed with Amber 20 [28], while trajectory analysis was done with CPPTRAJ [29]. The calculation of diffusion coefficients (D) based on the Einstein relation is:

$$2nD = \frac{MSD}{t}, \quad (1)$$

where n is the number of dimensions, t is time, and MSD is the mean square displacement [28][29].

## RESULT AND DISCUSSION

Chemical reactions in condensed systems are generally diffusion-controlled. According to the Stokes-Einstein law, the factors influencing ion diffusion include temperature, the viscosity of the medium ( $\eta^\circ$ ), and Stokes radius ( $r_s$ ), also known as hydrodynamic radius. The Stokes-Einstein equation is expressed as [30][31]:

$$D = \frac{kT}{6\pi\eta^\circ r_s}. \quad (2)$$

In the microscopic version of the Stokes-Einstein law, D can be calculated using the ion micro-viscosity ( $\eta_i$ ) and the ionic radius ( $r_i$ ), replacing  $\eta^\circ$  and  $r_s$ . In the context of aqueous solutions,  $\eta_i$  can be interpreted as the viscosity of water molecules within the first hydration shell, which can explain the influence of metal ions on the dynamics of water molecules in that hydration shell. If an ion has  $\eta_i > \eta^\circ$ , it acts as a structure maker for water molecules, whereas if  $\eta_i < \eta^\circ$ , it acts as a structure breaker [30].

Ions that act as structure makers attract more water molecules in their first and second coordination shells, resulting in a large  $r_s$  compared to ions that act as structure breakers. Structure-breaker ions' disruption of the hydration shell facilitates ion mobility; therefore, structure-breaker ions have higher mobility than structure-maker ions [18][30]. Particle transport in a fluid involves the movement of particles towards voids (free volume) that can accommodate those particles. Diffusion occurs due to the redistribution of free volume in

the fluid, which can be associated with the free volume created by the movement of water from the hydration shell to the bulk phase [32]. That indicates that the interaction between solutes and solvents is crucial in studying transport properties. The effect of temperature on the mobility of ions in aqueous solutions, including the interaction of ions with water molecules, can be studied through molecular dynamics simulations by explicitly including water molecules.

Based on the obtained  $25 \times 100$ -ns trajectories, we calculated the diffusion coefficients for all studied REE ions using Einstein's relation (Equation 1). As illustrated in Figure 1, the  $D$  values for  $\text{La}^{3+}$  are generally lower than those for other REE ions. This is likely due to the larger ionic radius of  $\text{La}^{3+}$ , which allows it to coordinate with more water molecules, as reported by D'Angelo et al. [20]. The range of average diffusion coefficients for these ions is from  $3.96 \times 10^{-6}$  to  $5.19 \times 10^{-6}$   $\text{cm}^2/\text{s}$ , with  $\text{Sm}^{3+}$  having the lowest diffusion coefficient and  $\text{Tb}^{3+}$  having the highest diffusion coefficient, as tabulated in **Table 1**. Overall, the  $D$  values for all REE ions tend to increase from  $\text{La}^{3+}$  to  $\text{Tb}^{3+}$ , corresponding to a decrease in ionic radii (**Figure 1**).

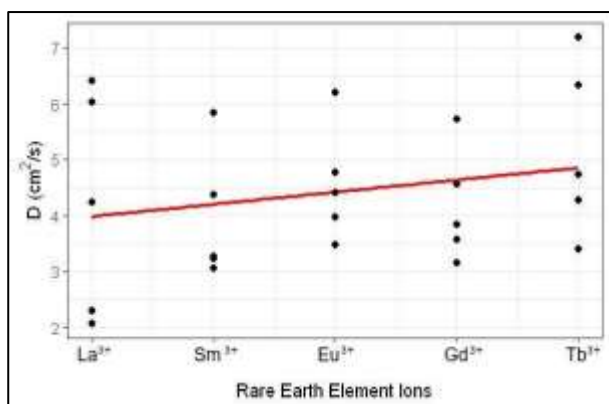


**Figure 1.** Dot plots of  $D$  for all studied REE ions. The REE ions include  $\text{La}^{3+}$ ,  $\text{Sm}^{3+}$ ,  $\text{Eu}^{3+}$ ,  $\text{Gd}^{3+}$ , and  $\text{Tb}^{3+}$ . Every data point was calculated from a 100-ns molecular dynamics simulation.

However, the Kruskal-Wallis test indicates no significant difference in diffusion coefficients among these ions ( $p = 0.5386$ ,  $\alpha = 5\%$ ), suggesting that diffusion is not a differentiating factor. Mixing in the extraction can diminish the diffusion as a rate-determining factor of the extraction. The influence of diffusion is limited to the area around the interface, specifically in the aqueous and organic stationary layers. If the thickness of these layers is very thin, then the diffusion factor becomes negligible and does not affect the extraction rate [33]. Thus, mixing can eliminate the

influence of metal ion diffusion as a differentiating factor in the separation among REE.

Our calculations are in agreement with the experiment of limiting diffusion coefficient of  $\text{Eu}^{3+}$ ,  $\text{Gd}^{3+}$ , and  $\text{Tb}^{3+}$  by Fourest et al. which also shows that  $\text{Gd}^{3+}$  has the lowest value [34]. Our calculations also show that  $\text{Gd}^{3+}$  has a narrow diffusion coefficient range compared to other ions. Although the 4f orbitals are not directly involved in coordination bonding [35], we suspect the electronic state of  $\text{Gd}^{3+}$  influences the dynamics of the surrounding water molecules. The electron configuration of  $\text{Gd}^{3+}$  in the ground state is  $[\text{Xe}]4f^7$ , having half-filled f orbitals with parallel spins. As a result,  $\text{Gd}^{3+}$  has symmetric f orbitals; therefore, it does not experience Jahn-Teller distortion. Therefore,  $\text{Gd}^{3+}$  can be a structure maker for the surrounding water molecules.

**Table 1.** Diffusion coefficients ( $D$ ) of  $\text{La}^{3+}$ ,  $\text{Sm}^{3+}$ ,  $\text{Eu}^{3+}$ ,  $\text{Gd}^{3+}$ , and  $\text{Tb}^{3+}$ . The  $D$  values tabulated are the mean and standard deviation from individual data points in Figure 1.  $D^\circ$  values from Mauerhofer et al. were calculated based on a microscopic version of the Stokes–Einstein law, whereas others were from open-end capillary experiments [30][34].

Ion	$D$ ( $10^{-6}$ $\text{cm}^2/\text{s}$ )		$D^\circ$ ( $10^{-6}$ $\text{cm}^2/\text{s}$ )	
	This work	Mauerhofer et al. [30]	Fourest et al. [34]	
$\text{La}^{3+}$	$4.21 \pm 2.02$	6.12	-	
$\text{Sm}^{3+}$	$3.96 \pm 1.17$	5.83	-	
$\text{Eu}^{3+}$	$4.57 \pm 1.04$	5.72	6.02	
$\text{Gd}^{3+}$	$4.17 \pm 1.01$	5.70	5.74	
$\text{Tb}^{3+}$	$5.19 \pm 1.54$	5.66	5.79	
p-value	0.5386	-	-	

$\text{Gd}^{3+}$  also possesses strong paramagnetic properties, originating from the presence of seven electrons in the f orbitals that have a very large spin magnetic moment. Under an external magnetic field,  $\text{Gd}^{3+}$  facilitates the exchange of water molecules between the  $\text{Gd}^{3+}$ - $\text{H}_2\text{O}$  coordination shell and water molecules in the bulk phase very effectively. Because of these properties,  $\text{Gd}^{3+}$  is used as a relaxation agent in magnetic resonance imaging (MRI) [5][6][7]. This suggests the concept of separating REE by utilizing an external magnetic field to create a significant difference in REE-water interactions, thereby resulting in a significant difference in diffusion coefficients.

Based on **Figure 1**, we conclude that, in general, the ion mobility of  $\text{REE}^{3+}$  tends to be influenced by  $r_i$  rather than  $r_s$ , unlike alkali metal

ions.  $\text{Sm}^{3+}$ ,  $\text{Eu}^{3+}$ ,  $\text{Gd}^{3+}$ , and  $\text{Tb}^{3+}$  have similar effective charges (2.92, 2.98, 2.96, and 2.98, respectively), so they will have similar charge densities [30]. Meanwhile, in alkali metal ions with +1 net charge, ion mobility is directly related to  $r_s$  rather than  $r_i$ . Ions with a large  $r_i$  have a low charge density, acting as structure breakers for water molecules around them. Conversely, ions with a small  $r_i$  have a high charge density, acting as structure makers [18][30].

## CONCLUSION

The diffusion coefficients of  $\text{La}^{3+}$ ,  $\text{Sm}^{3+}$ ,  $\text{Eu}^{3+}$ ,  $\text{Gd}^{3+}$ , and  $\text{Tb}^{3+}$  in water (water-n-hexane system) can be calculated by analyzing molecular dynamics simulation trajectories based on the Einstein relation. The Kruskal-Wallis test indicates no significant difference in diffusion coefficients among these ions, suggesting that diffusion is not a differentiating factor in the separation of these ions using extraction.

## ACKNOWLEDGEMENT

The authors acknowledge Universitas Padjadjaran for the financial support provided through the ALG funding scheme (Grant No. 1549/UN6.3.1/PT.00/2023) and the RPLK funding scheme (Grant No. 1549/UN6.3.1/PT.00/2023), which were awarded to AH and UMSS, respectively. We also would like to thank the Research Center for Molecular Biotechnology and Bioinformatics Universitas Padjadjaran and CV Biomolekul Data Sains (biomods.id) for the computer facilities.

## REFERENCES

- [1] J. Zhang, Z. Zhang, Y. Jiao, H. Yang, Y. Li, J. Zhang, and P. Gao, "The graphene/lanthanum oxide nanocomposites as electrode materials of supercapacitors", *Journal of Power Sources*, **419**, 99–105, 2019, doi: 10.1016/j.jpowsour.2019.02.059.
- [2] O.U. Osazuwa and C.K. Cheng, "Catalytic conversion of methane and carbon dioxide (greenhouse gases) into syngas over samarium-cobalt-trioxides perovskite catalyst", *Journal of Cleaner Production*, **148**, 202–211, 2017, doi: 10.1016/j.jclepro.2017.01.177.
- [3] K. Binnemans, "Interpretation of europium(III) spectra", *Coordination Chemistry Reviews*, **295**, 1–45, 2015, doi: 10.1016/j.ccr.2015.02.015.
- [4] J. Sun, B. Song, Z. Ye, and J. Yuan, "Mitochondria targetable time-gated luminescence probe for singlet oxygen based on a  $\beta$ -diketonate-europium complex", *Inorganic Chemistry*, **54**(24), 11660–11668, 2015, doi: 10.1021/acs.inorgchem.5b02458.
- [5] S. Aripionammal, S. Shalini, and S. N. Devi, "Structural, surface morphological, and low-temperature studies on gadolinium tri chloride ( $\text{GdCl}_3$ )", *Materials Today: Proceedings*, **35**, 39–43, 2021, doi: 10.1016/j.matpr.2019.05.406.
- [6] L. Blomqvist, G.F. Nordberg, V.M. Nurchi, and J. O. Aaseth, "Gadolinium in medical imaging—usefulness, toxic reactions, and possible countermeasures—a review", *Biomolecules*, **12**, 742, 2022, doi: 10.3390/biom12060742.
- [7] P. Eriksson. *Cerium oxide nanoparticles and gadolinium integration: synthesis, characterization and biomedical applications*. Linköping: Linköping University Electronic Press, 2019.
- [8] H. Li and T. J. Meade, "Molecular magnetic resonance imaging with Gd(III)-based contrast agents: challenges and key advances", *Journal of the American Chemical Society*, **141**(43), 17025–17041, 2019, doi: 10.1021/jacs.9b09149.
- [9] B. Poornaprakash, U. Chalapathi, Y. Suh, S. V.P. Vattikuti, M.S.P. Reddy, and S.-H. Park, "Terbium-doped ZnS quantum dots: Structural, morphological, optical, photoluminescence, and photocatalytic properties", *Ceramics International*, **44** (10), 11724–11729, 2018, doi: 10.1016/j.ceramint.2018.03.250.
- [10] P. Moeyaert, M. Miguiditchian, M. Masson, B. Dinh, X. Hérès, S. De Sio, and C. Sorel, "Experimental and modelling study of ruthenium extraction with tri-n-butylphosphate in the purex process", *Chemical Engineering Science*, **158**, 580–586, 2017, doi: 10.1016/j.ces.2016.10.035.
- [11] G. Benay and G. Wipff, "Liquid-liquid extraction of uranyl by TBP: The TBP and ions models and related interfacial features revisited by MD and PMF simulations", *J. Phys. Chem. B*, **118**(11), 3133–3149, 2014, doi: 10.1021/jp411332e.
- [12] W. Wang, Y. Pranolo, and C.Y. Cheng, "Recovery of scandium from synthetic red mud leach solutions by solvent extraction with D2EHPA", *Separation and Purification*

- Technology*, **108**, 96–102, 2013, doi: 10.1016/j.seppur.2013.02.001.
- [13] W.-S. Chen, K.-W. Tien, L.-P. Wang, C.-H. Lee, and Y.-F. Chung, “Recovery of gallium from simulated gas waste etching solutions by solvent extraction”, *Sustainability*, **12**(5), 1765, 2020, doi: 10.3390/su12051765.
- [14] C. Tunsu, C. Ekberg, M. Foreman, and T. Retegan, “Studies on the solvent extraction of rare earth metals from fluorescent lamp waste using cyanex 923”, *Solvent Extraction and Ion Exchange*, **32**(6), 650–668, 2014, doi: 10.1080/07366299.2014.925297.
- [15] K. Shimojo, N. Aoyagi, T. Saito, H. Okamura, F. Kubota, M. Goto, and H. Naganawa, “Highly efficient extraction separation of lanthanides using a diglycolamic acid extractant”, *Anal. Sci.*, **30**(2), 263–269, 2014, doi: 10.2116/analsci.30.263.
- [16] A.U. Chowdhury, L. Lin, and B. Doughty, “Hydrogen-bond-driven chemical separations: elucidating the interfacial steps of self-assembly in solvent extraction”, *ACS Appl. Mater. Interfaces*, **12**(28), 32119–32130, 2020, doi: 10.1021/acsami.0c06176.
- [17] Z. Liu, X. Ren, R. Tan, Z. Chai, and D. Wang, “Key factors determining efficiency of liquid–liquid extraction: Implications from molecular dynamics simulations of biphasic behaviors of CyMe<sub>4</sub>-BTPPhen and its Am(III) complexes”, *J. Phys. Chem. B*, **124**(9), 1751–1766, 2020, doi: 10.1021/acs.jpcc.9b08447.
- [18] P.W. Atkins, J. de Paula, and J.J. Keeler, *Atkins’ physical chemistry*, Eleventh edition. Oxford New York: Oxford University Press, 2018.
- [19] A. Zhou, S. Ju, S. Koppala, L. Xu, J. Peng, and S. Tian, “Extraction of In<sup>3+</sup> and Fe<sup>3+</sup> from sulfate solutions by using a 3D-printed ‘Y’-shaped microreactor”, *Green Processing and Synthesis*, **8**(1), 163–171, 2019, doi: 10.1515/gps-2018-0045.
- [20] P. D’Angelo, A. Zitolo, V. Migliorati, G. Chillemi, M. Duvail, P. Vitorge, S. Abadie, and R. Spezia., “Revised ionic radii of lanthanoid(III) ions in aqueous solution”, *Inorg. Chem.*, **50**(10), 4572–4579, 2011, doi: 10.1021/ic200260r.
- [21] P.P. Passler and B. M. Rode, “The properties of trivalent praseodymium, neodymium, promethium and samarium ions in water: A quantum mechanical molecular dynamics study”, *Chemical Physics Letters*, **642**, 12–16, 2015, doi: 10.1016/j.cplett.2015.10.065.
- [22] L. Martínez, R. Andrade, E.G. Birgin, and J. M. Martínez, “PACKMOL: A package for building initial configurations for molecular dynamics simulations”, *J. Comput. Chem.*, vol. 30, no. 13, pp. 2157–2164, Oct. 2009, doi: 10.1002/jcc.21224.
- [23] B.M. Allen, P.K. Predecki, and M. Kumosa, “Integrating open-source software applications to build molecular dynamics systems”, *J. Comput. Chem.*, **35**(9), 756–764, 2014, doi: 10.1002/jcc.23537.
- [24] W.L. Jorgensen, J. Chandrasekhar, J.D. Madura, R.W. Impey, and M.L. Klein, “Comparison of simple potential functions for simulating liquid water”, *J. Chem. Phys.*, **79**(2), 926–935, 1983, doi: 10.1063/1.445869.
- [25] S. Mamatkulov and N. Schwierz, “Force fields for monovalent and divalent metal cations in TIP3P water based on thermodynamic and kinetic properties”, *The J. Chem. Phys.*, **148**(7), 074504, 2018, doi: 10.1063/1.5017694.
- [26] X. He, V.H. Man, W. Yang, T.S. Lee, and J. Wang, “A fast and high-quality charge model for the next generation general AMBER force field”, *J. Chem. Phys.*, **153**(11), 1–11, 2020, doi: 10.1063/5.0019056.
- [27] K.G. Sprenger, V.W. Jaeger, and J. Pfandner, “The general AMBER force field (GAFF) can accurately predict thermodynamic and transport properties of many ionic liquids”, *J. Phys. Chem. B*, **119**(18), 5882–5895, 2015, doi: 10.1021/acs.jpcc.5b00689.
- [28] D.A. Case, H.M. Aktulga, K. Belfon, I.Y. Ben-Shalom, J.T. Berryman, S.R. Brozell, D.S. Cerutti, T.E. Cheatham, III, G.A. Cisneros, V.W.D. Cruzeiro, T.A. Darden, N. Forouzes, G. Giambasu, T. Giese, M.K. Gilson, H. Gohlke, A.W. Goetz, J. Harris, S. Izadi, S.A. Izmailov, K. Kasavajhala, M.C. Kaymak, E. King, A. Kovalenko, T. Kurtzman, T.S. Lee, P. Li, C. Lin, J. Liu, T. Luchko, R. Luo, M. Machado, V. Man, M. Manathunga, K.M. Merz, Y. Miao, O. Mikhailovskii, G. Monard, H. Nguyen, K.A. O’Hearn, A. Onufriev, F. Pan, S. Pantano, R. Qi, A. Rahnamoun, D.R. Roe, A. Roitberg, C. Sagui, S. Schott-Verdugo, A. Shajan, J. Shen, C.L. Simmerling, N.R. Skrynnikov, J. Smith, J. Swails, R.C. Walker, J. Wang, J.

- Wang, H. Wei, X. Wu, Y. Wu, Y. Xiong, Y. Xue, D.M. York, S. Zhao, Q. Zhu, and P.A. Kollman, *Amber 2021*. San Francisco: University of California, 2021.
- [29] D.R. Roe and T.E. Cheatham, "PTRAJ and CPPTRAJ: Software for processing and analysis of molecular dynamics trajectory data", *J. Chem. Theory Comput.*, **9**(7), 3084–3095, 2013, doi: 10.1021/ct400341p.
- [30] E. Mauerhofer, K.P. Zhernosekov, and F. Rösch, "Limiting transport properties of lanthanide and actinide ions in pure water", *Radiochimica Acta*, **91**(8), 473–478, 2003, doi: 10.1524/ract.91.8.473.20009.
- [31] F. Puosi, A. Pasturel, N. Jakse, and D. Leporini, "Communication: Fast dynamics perspective on the breakdown of the Stokes-Einstein law in fragile glassformers", *J. Chem. Phys.*, **148**(13), 131102, 2018, doi: 10.1063/1.5025614.
- [32] H. Liu, "Free volume power law for transport properties of hard sphere fluid", *Journal of Applied Physics*, **129**(4), 044701, 2021, doi: 10.1063/5.0039615.
- [33] P.R. Danesi, R. Chiarizia, and C.F. Coleman, "The kinetics of metal solvent extraction", *CRC Critical Reviews in Analytical Chemistry*, **10**(1), 1–126, 1980, doi: 10.1080/10408348008542724.
- [34] B. Fourest, J. Duplessis, and F. David, "Comparison of Diffusion Coefficients and Hydrated Radii for some Trivalent Lanthanide and Actinide Ions in Aqueous Solution", *Radiochimica Acta*, **36**(4), 191–196, 1984, doi: 10.1524/ract.1984.36.4.191.
- [35] W.W. Lukens, M. Speldrich, P. Yang, T.J. Duignan, J. Autschbach, and P. Kögerler, "The roles of 4f- and 5f-orbitals in bonding: a magnetochemical, crystal field, density functional theory, and multi-reference wavefunction study", *Dalton Trans.*, **45**(28), 11508–11521, 2016, doi: 10.1039/C6DT00634E.